PHYSICAL REVIEW B **94**, 140502(R) (2016)

First-principles approach to thin superconducting slabs and heterostructures

Gábor Csire,[1] Stephan Schönecker,[2] and Balázs Újfalussy[1]

[1]*Institute for Solid State Physics and Optics, Wigner Research Centre for Physics, Hungarian Academy of Sciences, P.O. Box 49, H-1525 Budapest, Hungary*

[2]*Applied Materials Physics, Department of Materials Science and Engineering, Royal Institute of Technology, SE-10044 Stockholm, Sweden*

(Received 4 July 2016; published 10 October 2016)

We present a fully first-principles method for superconducting thin films. The layer dependent phonon spectrum is calculated to determine the layer dependence of the electron-phonon coupling for such systems, which is coupled to the Kohn–Sham–Bogoliubov–de Gennes equations, and it is solved in a parameter-free way. The theory is then applied to different surface facets of niobium slabs and to niobium-gold heterostructures. We investigate the dependence of the transition temperature on the thickness of the slabs and the inverse proximity effect observed in thin superconducting heterostructures.

DOI: 10.1103/PhysRevB.94.140502

I. INTRODUCTION

Thin film superconductivity has been a subject of great scientific interest since the 1950's [1–5]. The development of nanotechnology has led to renewed interest in this topic [6–14] due to possible technological applications in superconducting nanodevices. Theoretically, it is entirely possible that in thin (few nanometers thick) slabs a large electron-phonon coupling can lead to superconductivity well above the bulk transition temperature. For such superconducting heterostructures an inverse proximity effect was also observed [6]: A nonsuperconducting metal overlayer on a superconducting thin film increases the critical temperature T_c. This is in strong contrast to the case of thick (compared to the coherence length) superconducting films, where the metallic overlayer decreases T_c [15–17]. In this Rapid Communication, the main focus is how the material specific, intrinsic superconducting properties (which are essential for technological applications) change as a function of thickness. In the case of thin superconducting films, the electron-phonon interaction may change significantly compared to bulk, which can lead to many new and interesting effects. To properly describe such a situation, a fully *ab initio* approach is needed, which takes into account the changes in the electronic structure and in the phonon spectrum. However, the simultaneous treatment of vibrational and electronic degrees of freedom on the same level leads to complications which are very difficult to overcome. Here we propose a simplified treatment, where both spectra are calculated separately on a first-principles level and the results are combined. The theory is applied to different surface facets of niobium slabs and to niobium-gold heterostructures.

II. METHODS

The density functional theory (DFT) for superconductors yields the Kohn–Sham–Bogoliubov–de Gennes (KSBdG) equations [18–20] by introducing the $\chi(\vec{r}) = \langle \Psi_\downarrow(\vec{r})\Psi_\uparrow(\vec{r})\rangle$ anomalous density as an additional density, analogous to the magnetization in spin-polarized DFT theory. In the case of multilayer systems, the self-consistent solution of these equations can be obtained in terms of the screened Korringa-Kohn-Rostoker (SKKR) method (see Ref. [21]), where the retarded Green's function $\{G^{ab,+}_{IJ,LL'}(\varepsilon,\vec{r},\vec{k}_{||})\}$ is the fundamental quantity of interest. Here, a,b refer to the electron-hole components, I,J are the layer indices, and $L = (l,m)$ is a composite angular momentum index. Physical quantities, such as the $\rho_I(\vec{r})$ charge and $\chi_I(\vec{r})$ anomalous densities, can be calculated from the layer diagonal Green's function, as described in Ref. [21].

For self-consistent calculations one can use the parametrization for the exchange energy introduced by Suvasini *et al.* [22],

$$E_{\mathrm{xc},I}[\rho_I,\chi_I] = E^0_{\mathrm{xc},I}[\rho_I] - \int \chi^*_I(\vec{r})\Lambda_I\chi_I(\vec{r})d\vec{r}, \qquad (1)$$

where $E^0_{\mathrm{xc},I}[\rho_I]$ is the usual exchange-correlation energy for electrons in the normal state and Λ_I describes the strength of the electron-phonon interaction for layer I. Each layer is assumed to be chemically homogeneous, but any two distinct layers can, in principle, describe different material constituents.

The approximation Eq. (1) to the exchange-correlation potential takes into account the electron-phonon interaction via a single layer dependent parameter. This parameter can be estimated from the λ_I electron-phonon coupling constant as $\Lambda_I = \lambda_I/D_I(E_F)$, where $D_I(E_F)$ is the density of states (DOS) at the Fermi energy for layer I. Furthermore, the electron-phonon coupling constant can be calculated as [23]

$$\lambda_I = \frac{D_I(E_F)\langle g^2_I\rangle}{M_I\langle\omega^2_I\rangle}, \qquad (2)$$

where M_I is the atomic mass, and $D_I(E_F)\langle g^2_I\rangle$ is the McMillan-Hopfield parameter. One can immediately recall that various theories [24–26] have been worked out in the literature to calculate the terms in the above expression. A purely electronic calculation leads to the McMillan-Hopfield parameter via the Gaspari-Győrffy formula [24], which is based on the following assumptions: (i) The atomic potentials are spherically symmetric, (ii) every special influence of the shape of the Fermi surface is neglected, and (iii) small displacements in the atomic potential can be approximated by a rigid shift. The other important parameter used to evaluate Eq. (2) is the average of the square of the phonon frequency,

$\langle\omega_I^2\rangle$, which can be calculated based on the formula [23]

$$\langle\omega_I^2\rangle \approx \frac{\int d\omega\omega F_I(\omega)}{\int d\omega \frac{1}{\omega} F_I(\omega)}, \tag{3}$$

where $F_I(\omega)$ is the phonon DOS for layer I. Even at this point one can notice that a larger McMillan-Hopfield parameter, the softening of $\langle\omega_I^2\rangle$, will result in a larger electron-phonon coupling.

Our phonon calculations are based on relaxed slab geometries, and interlayer relaxations are assumed for all interlayer distances perpendicular to the surface facets with a fixed in-plane lattice parameter. The first-principles calculation of the dynamical properties of lattices requires knowledge of the interatomic forces. We determine the force constant matrix for bulk, slabs, and heterostructures in the framework of density functional perturbation theory [27] as implemented in the Vienna *ab initio* simulation package (VASP) [28] and employing PHONOPY [29] to compute the dynamical matrix and layer resolved phonon DOS. Once the layer dependent phonon spectrum has been obtained, the layer dependent electron-phonon coupling constants can be calculated based on Eq. (2) and, consequently, the KSBdG equations can be solved self-consistently for finite temperatures with the SKKR method. These self-consistent calculations are carried out within the atomic sphere approximation with an angular momentum cutoff of $l_{\max} = 2$. In order to determine the superconducting transition temperature, one needs to find the critical temperature where the spectrum of the KSBdG Hamiltonian does not give a gap.

In what follows, we choose niobium as the test bed and primary target of our numerical investigations. To verify the theory, we first calculated the electron-phonon coupling and the critical temperature for bulk Nb, and obtained $\lambda = 0.86$ and $T_c = 11.3$ K. Based on the Gaspari-Győrffy theory and using the augmented plane wave method, for Nb, $\lambda = 0.88$ was obtained by Klein and Papaconstantopoulos [30]. In Ref. [20] a multicomponent DFT for the combined system of electrons and nuclei with different hybrid functionals led to critical temperatures in the range of 8.4–9.5 K, while the known experimental bulk values for Nb are [30] $\lambda^{(\text{expt})} = 0.82$ and $T_c^{(\text{expt})} = 9.2$ K. It can be seen that our results are rather similar to the results of other authors regarding the electron-phonon interaction and the critical temperature is slightly overestimated as compared to experiments, which is, despite the simplicity of the used exchange-correlation energy, still not far from the experimental value. It is worth mentioning here that in the case of niobium, phonon retardation effects play an important role, therefore, it should be treated in the strong-coupling limit. In our theory, the anomalous density $\chi_I(\vec{r})$ influences the effective potential $V_{\text{eff},I}(\vec{r})$ via the density $\rho_I(\vec{r})$, which is the analogy of the self-energy correction to the Eliashberg equations [31] and therefore may be regarded as a strong-coupling effect.

III. RESULTS

Now we are ready to apply the method to niobium slabs, and niobium-gold heterostructures. It should be noted that throughout this Rapid Communication we neglect the effect of a substrate which could, in principle, modify the results quantitatively, but should not alter the basic physics and would just lead to numerical complications in the calculation of the phonon spectrum. In the case of a Nb slab, the calculations were performed for three, six, nine, 12, and 15 layers of Nb. We choose two facets for our studies: the open (100) surface facet, because it is the most stable surface facet, and a contrasting close-packed one, namely, the (110) facet, which has a slightly higher surface energy.

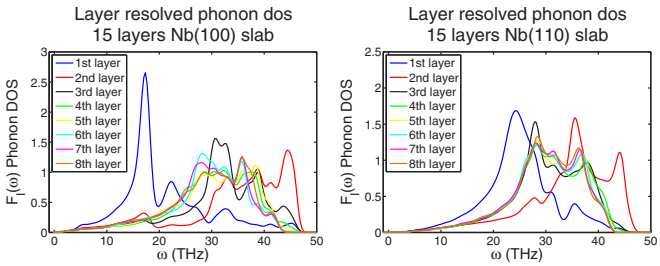

FIG. 1. Layer resolved phonon DOS of a 15 layer Nb slab for bcc(100) (left panel) and bcc(110) (right panel). The first layer is the surface layer, the second layer is the subsurface layer, . . . , and the eighth layer is the bulklike center of the slab.

The results obtained for the McMillan-Hopfield parameter, the average phonon frequency and the electron-phonon interaction, are presented in a graphical form with a stacked bar chart in Fig. 2. Since the slabs are symmetric with respect to the center of the sample, we plot the results only from the surface layer to the middle of the sample. In Fig. 1 the phonon DOS is shown for both Nb(100) and Nb(110) slabs consisting of 15 atomic layers. It can be observed that as one approaches the middle of the sample, the phonon DOS converges towards the bulk DOS. A faster convergence was obtained in the case of the electron DOS. It can be seen that on the surface of the bcc(100) slab, the phonon DOS is dominated by low frequency states, therefore, the $\langle\omega_I^2\rangle$ becomes significantly smaller just on the first surface layer (see Fig. 2). This effect can also be observed for the bcc(110) slab but it is not as pronounced, and is mostly compensated by the subsurface layer where the phonon DOS is dominated by high frequency states. As a consequence, for the bcc(100) surface facet, the McMillan-Hopfield parameter increases on approaching the surface, which is in sharp contrast to the bcc(110) surface facet where the McMillan-Hopfield parameter fluctuates around its bulk value for all layers. At the (100) surface, both the electron and the phonon parts enlarge the electron-phonon coupling significantly beyond the bulk value. At the subsurface layer, the electron-phonon coupling becomes smaller because of the larger $\langle\omega_I^2\rangle$, and as we approach the middle of the sample its value converges to the bulk value. In the case of the bcc(110) slab, the electron-phonon coupling changes similarly to the bcc(100) slab, however, an important difference is that on the surface the electron-phonon coupling is not as large.

Once we know the electron-phonon interaction parameters for all layers, we can proceed and solve the KSBdG equations self-consistently for various temperatures. In the case of $T = 0$ K, we find that the superconducting gap has a layer dependence, which follows the layer dependence of the λ_I electron-phonon coupling parameter. However, when the

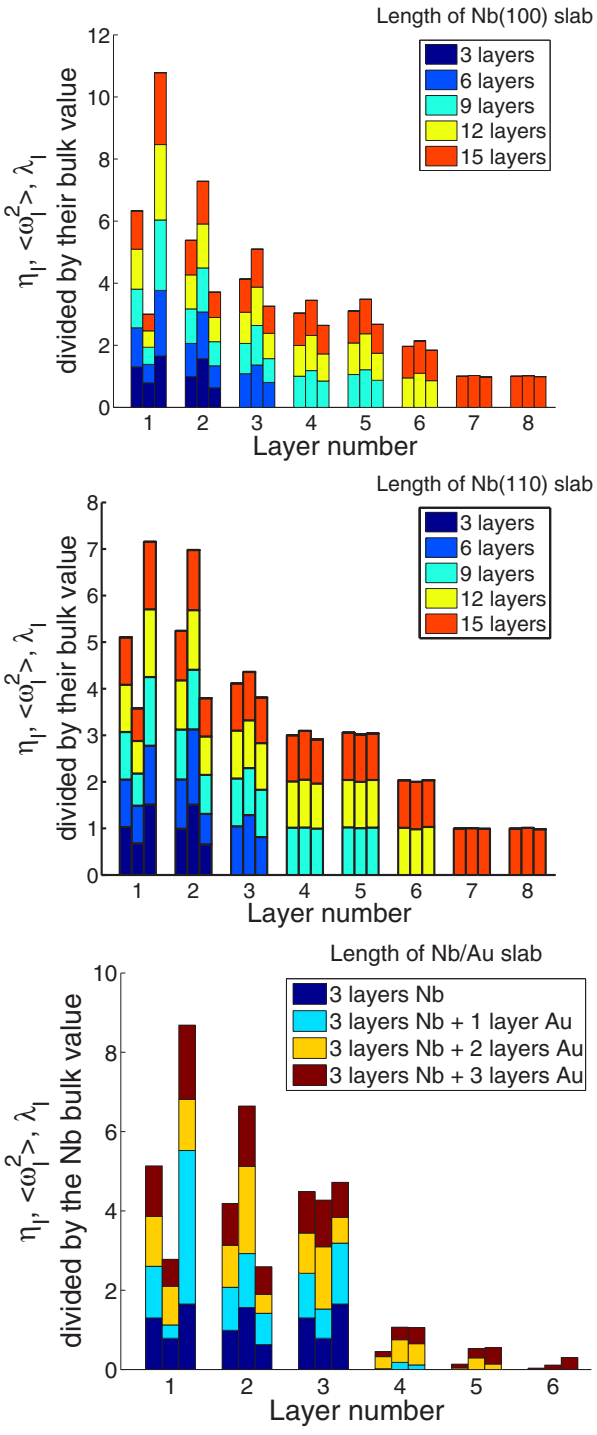

FIG. 2. $\eta_I = D_I(E_F)\langle g_I^2\rangle/M_I$, $\langle\omega_I^2\rangle$, λ_I—normalized with the Nb bulk value—are shown in the stacked bar charts (the actual value is always added to the sum of the other data sets), respectively, in each bar, for different lengths of Nb(100) (top panel), Nb(110) (middle panel), and Nb/Au (bottom panel) slabs, where one, two, and three layers of Au were added on three Nb layers.

KSBdG equations are solved for finite temperatures, it is found that in all layers the superconducting gaps disappear at the same critical temperature. This means that a layer, which has a larger electron-phonon coupling parameter, strengthens the superconducting properties of the other layers with smaller

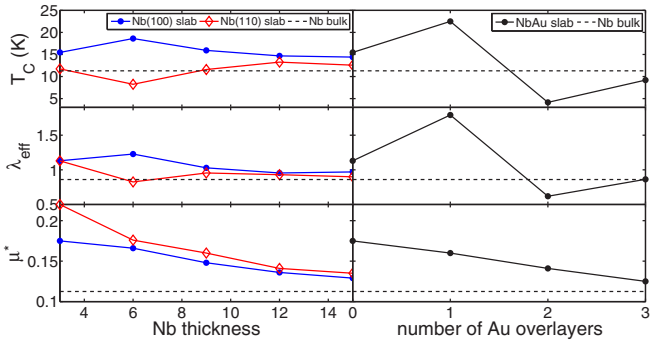

FIG. 3. The critical temperature (T_c), effective electron-phonon coupling (λ_{eff}), and Coulomb repulsion (μ^*) as a function of the thickness of Nb(100) (blue line, solid symbol) and Nb(110) (red line, open symbol) slabs (left panels), and Nb/Au slabs (right panels).

electron-phonon coupling via the proximity effect [32]. Formally, this is very similar to the case of MgB_2's two-band system [33], where the two superconducting gaps have the same critical temperature only if there is an interband coupling.

In Fig. 3 (top left panel) it can be seen that the critical temperature of the Nb(100) slab is well above the bulk critical temperature (with a maximum at the six layer thick Nb slab), which is clearly due to the larger electron-phonon coupling on the surface. Not surprisingly, the Nb(110) slab's critical temperature is always lower than in the case of the Nb(100) slab. In order to gain a deeper understanding of the changes in the critical temperature as a function of thickness, it is interesting to look at other properties of the superconducting slabs, such as μ^*, the effective Coulomb repulsion. The μ^* is a fundamental quantity in the theory of superconductivity, related to the correlation effects due to the Coulomb repulsion. Usually, it is treated as an adjustable parameter, but based on the previous results, it is possible to estimate it in thin film systems. For a strong-coupling superconductor such as Nb, T_c can be calculated from the McMillan formula [23], which depends on the Debye temperature Θ_D, the effective electron-phonon coupling λ_{eff}, and the μ^*. If the values of λ_I are known, it is possible to calculate λ_{eff} as [34]

$$\lambda_{\text{eff}} = \frac{\sum_I \lambda_I D_I(E_F)}{\sum_I D_I(E_F)}, \tag{4}$$

where I is a layer index. Θ_D can be obtained from the phonon spectrum. Thus μ^* can be calculated by equating the previously obtained value of T_c to the McMillan formula. The results are shown in Fig. 3 (left panels), where one can see that the effective Coulomb repulsion is decreasing as a function of the niobium thickness. This is probably due to the fact that for thicker slabs the electrons have more degrees of freedom. It is also worth mentioning that, as it can be seen in Fig. 3, the superconducting transition temperature has a rather similar dependence on the thickness of the slab as the above defined λ_{eff}.

The more important and more studied systems are the superconducting thin film heterostructures. Due to the scarcity of experimental studies of such systems, we choose to investigate the Nb/Au heterostructure, mostly because the thick film version was already investigated in Refs. [15–17].

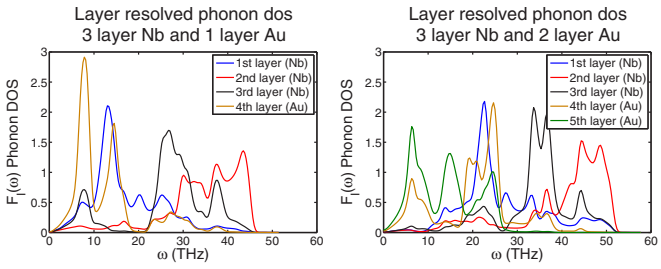

FIG. 4. Layer resolved phonon DOS for the following heterostructures: one Au layer (left panel) and two Au layers (right panel) on three Nb layers.

Here, one, two, and three layers of gold were added to three layers of Nb. We assumed bcc epitaxial growth for the gold overlayers, and thus the bcc(100) lattice structure is investigated. The layer resolved phonon DOS is shown for one and two gold overlayers in Fig. 4. It can be seen that in the case of a single gold overlayer the phonon spectrum is dominated by low frequencies both in the case of the Au overlayer and the surface niobium layer (which is on the other side of the slab), therefore, the $\langle\omega_I^2\rangle$ becomes smaller on these layers. This effect tends to increase the electron-phonon coupling. However, the McMillan-Hopfield parameter is also smaller for the gold layers, as it can be seen in Fig. 2 (bottom panel), since the electronic DOS at the Fermi level is smaller and also the mass of a gold atom is almost twice as large as the mass of a niobium atom. Together these latter factors would act to reduce the electron-phonon coupling in the gold layers. All these factors are not present or not as pronounced when the gold coverage increases to two or more layers. However, for the three layer Nb/one layer Au heterostructure, the electron-phonon coupling in the surface Nb layer is much larger than any one layer in any other presently investigated heterostructures or slabs. The net result is an overall increased electron-phonon coupling and (as we will see further down) an increased T_c in the case of a single Au covered Nb thin film. The results for the different heterostructures are summarized in Fig. 2 (bottom panel).

Again, knowing the electron-phonon interaction parameters, similar calculations were performed as in the case of the niobium slab to obtain the critical temperature, the effective electron-phonon coupling, and the effective Coulomb repulsion as a function of the thickness of the gold coverage. In Fig. 3 (right panel) we can observe the inverse proximity effect similarly as it was found experimentally in the Pb/Ag heterostructure in Ref. [6] or in a similar Nb/Au/Nb junction in Ref. [35]. The superconducting transition temperature T_c increases by adding only one gold overlayer to a niobium slab, however, adding two layers of gold decreases the T_c. This result is now well understood based on the previous result regarding the electron-phonon interaction. Bourgeois *et al.* [6] suggested that there is a competition between the Coulomb effects and the classical proximity effect. Indeed, in Fig. 3 (right panel) it can be seen that with increasing the number of gold overlayers, the effective Coulomb repulsion decreases, which can cause an increase in the critical temperature. Nevertheless, based on Fig. 3 (right panel), we would rather conclude that the main effect which creates the inverse proximity effect is due to the enhanced electron-phonon coupling in the overlayer. The behavior of the electron-phonon interaction appears to primarily influence T_c in other thicknesses as well, overriding the changes coming from the Coulomb repulsion.

IV. SUMMARY

In this Rapid Communication a first-principles approach was presented to investigate superconducting slabs and S/N heterostructures. In essence, the scheme of calculation presented here requires the solution of two separate problems: solving the KSBdG equations and constructing exchange functionals. In Ref. [21] the SKKR method was generalized for the superconducting state and now a simple scheme was constructed to obtain a simple approximation for the exchange functional. The method was applied to niobium and niobium-gold slabs. In the case of freestanding Nb bcc(100) slabs we have found that the McMillan-Hopfield parameter is larger, and the $\langle\omega_I^2\rangle$ frequency is smaller on the surface of the Nb, which results in large electron-phonon coupling for the surface. As a consequence, the critical temperature is above the bulk value. For the Nb(110) slab the McMillan-Hopfield parameters are almost constant, and the $\langle\omega_I^2\rangle$ frequencies show a behavior similar to that of the Nb(100) surface facet. Therefore, the critical temperature is oscillating around the bulk value. While presently there is no first-principles way to directly calculate the effective Coulomb repulsion parameter (μ^*), a procedure was developed to estimate this parameter via the McMillan formula. We also studied the properties of thin Nb/Au heterostructures where we could observe the inverse proximity effect for which a first-principles based explanation was found.

ACKNOWLEDGMENTS

Financial support by the Hungarian National Research, Development and Innovation Office under Contract No. K115632, the Swedish Research Council, the Swedish Foundation for Strategic Research, and the Swedish Foundation for International Cooperation in Research and Higher Education is gratefully acknowledged. The Swedish National Infrastructure for Computing is acknowledged for providing computational facilities. The authors would like to thank the useful discussions József Cserti.

[1] W. Buckel and R. Hilsch, Z. Phys. **138**, 109 (1954).
[2] J. M. Blatt and C. J. Thompson, Phys. Rev. Lett. **10**, 332 (1963).
[3] B. Abeles, R. W. Cohen, and G. W. Cullen, Phys. Rev. Lett. **17**, 632 (1966).
[4] M. Strongin, R. S. Thompson, O. F. Kammerer, and J. E. Crow, Phys. Rev. B **1**, 1078 (1970).
[5] D. B. Haviland, Y. Liu, and A. M. Goldman, Phys. Rev. Lett. **62**, 2180 (1989).

[6] O. Bourgeois, A. Frydman, and R. C. Dynes, Phys. Rev. Lett. **88**, 186403 (2002).
[7] Y. Guo, Science **306**, 1915 (2004).
[8] M. M. Özer, J. R. Thompson, and H. H. Weitering, Nat. Phys. **2**, 173 (2006).
[9] D. Eom, S. Qin, M.-Y. Chou, and C. K. Shih, Phys. Rev. Lett. **96**, 027005 (2006).
[10] C. Brun, I.-P. Hong, F. Patthey, I. Y. Sklyadneva, R. Heid, P. M. Echenique, K. P. Bohnen, E. V. Chulkov, and W.-D. Schneider, Phys. Rev. Lett. **102**, 207002 (2009).
[11] K. Wang, X. Zhang, M. M. T. Loy, T.-C. Chiang, and X. Xiao, Phys. Rev. Lett. **102**, 076801 (2009).
[12] S. Qin, J. Kim, Q. Niu, and C.-K. Shih, Science **324**, 1314 (2009).
[13] T. Zhang, P. Cheng, W.-J. Li, Y.-J. Sun, G. Wang, X.-G. Zhu, K. He, L. Wang, X. Ma, X. Chen, Y. Wang, Y. Liu, H.-Q. Lin, J.-F. Jia, and Q.-K. Xue, Nat. Phys. **6**, 104 (2010).
[14] C. Delacour, L. Ortega, M. Faucher, T. Crozes, T. Fournier, B. Pannetier, and V. Bouchiat, Phys. Rev. B **83**, 144504 (2011).
[15] H. Yamazaki, N. Shannon, and H. Takagi, Phys. Rev. B **73**, 094507 (2006).
[16] H. Yamazaki, N. Shannon, and H. Takagi, Phys. Rev. B **81**, 094503 (2010).
[17] G. Csire, J. Cserti, I. Tüttő, and B. Újfalussy, Phys. Rev. B **94**, 104511 (2016).
[18] L. N. Oliveira, E. K. U. Gross, and W. Kohn, Phys. Rev. Lett. **60**, 2430 (1988).
[19] M. Lüders, M. A. L. Marques, N. N. Lathiotakis, A. Floris, G. Profeta, L. Fast, A. Continenza, S. Massidda, and E. K. U. Gross, Phys. Rev. B **72**, 024545 (2005).
[20] M. A. L. Marques, M. Lüders, N. N. Lathiotakis, G. Profeta, A. Floris, L. Fast, A. Continenza, E. K. U. Gross, and S. Massidda, Phys. Rev. B **72**, 024546 (2005).
[21] G. Csire, B. Újfalussy, J. Cserti, and B. Győrffy, Phys. Rev. B **91**, 165142 (2015).
[22] M. B. Suvasini, W. M. Temmerman, and B. L. Gyorffy, Phys. Rev. B **48**, 1202 (1993).
[23] W. L. McMillan, Phys. Rev. **167**, 331 (1968).
[24] G. D. Gaspari and B. L. Gyorffy, Phys. Rev. Lett. **28**, 801 (1972).
[25] S. Y. Savrasov, D. Y. Savrasov, and O. K. Andersen, Phys. Rev. Lett. **72**, 372 (1994).
[26] S. Y. Savrasov, Phys. Rev. B **54**, 16470 (1996).
[27] S. Baroni, S. de Gironcoli, A. D. Corso, and P. Giannozzi, Rev. Mod. Phys. **73**, 515 (2001).
[28] G. Kresse and J. Furthmüller, Phys. Rev. B **54**, 11169 (1996).
[29] A. Togo and I. Tanaka, Scr. Mater. **108**, 1 (2015).
[30] B. M. Klein and D. A. Papaconstantopoulos, Phys. Rev. Lett. **32**, 1193 (1974).
[31] P. B. Allen and B. Mitrović, in *Solid State Physics* (Elsevier, Amsterdam, 1983), pp. 1–92.
[32] G. Csire, J. Cserti, and B. Újfalussy, J. Phys.: Condens. Matter (to be published).
[33] E. J. Nicol and J. P. Carbotte, Phys. Rev. B **71**, 054501 (2005).
[34] P. G. De Gennes, Rev. Mod. Phys. **36**, 225 (1964).
[35] H. Yamazaki, N. Shannon, and H. Takagi, arXiv:1602.05790.